A&A, 703, L13 (2025)
https://doi.org/10.1051/0004-6361/202557347

Astronomy & Astrophysics

LETTER TO THE EDITOR

The changing look of the neutrino-emitter blazar candidate 5BZQ J1243+4043

Alessandra Azzollini[1,2,⋆], Sara Buson[1,2], and Alexis Coleiro[3]

[1] Julius-Maximilians-Universität Würzburg, Fakultät für Physik und Astronomie, Institut für Theoretische Physik und Astrophysik, Lehrstuhl für Astronomie, Emil-Fischer-Str. 31, D-97074 Würzburg, Germany
[2] Deutsches Elektronen-Synchrotron DESY, Platanenallee 6, 15738 Zeuthen, Germany
[3] Université Paris Cité, CNRS, Astroparticule et Cosmologie, F-75013 Paris, France

Received 21 September 2025 / Accepted 28 October 2025

ABSTRACT

Context. In recent years, changing-look blazars have called the traditional view of BL Lacs-flat spectrum radio quasars into question within the empirical classification of blazars. Based on the intensity of the optical spectral lines, they appear to transition between the two classes over time.
Aims. We focus on the blazar 5BZQ J1243+4043, recently proposed as a promising candidate for the emission of high-energy neutrinos observed by the IceCube Neutrino Observatory and reported as a changing-look blazar in the literature. We study the spectral properties of this blazar, inferring its radiation field and accretion regime properties across different epochs.
Methods. This study presents new optical spectroscopy observations of 5BZQ J1243+4043 taken with the Gran Telescopio Canarias. We used this new dataset and two optical spectra available from the literature to investigate the continuum and line emissions and pinpoint the physical properties of the source. In particular, we used the emission lines to probe the accretion regime.
Results. The newly collected data for 5BZQ J1243+4043 shows broad emission lines, consistent with the spectrum of the first epoch and the redshift $z = 1.5181 \pm 0.0002$ known from the literature. For the second epoch, the spectrum appears featureless and so, we placed limits on the emission lines and related physical properties. We observed spectral variability for both the continuum and line emissions among the three spectra. Nonetheless, the accretion properties of the blazar generally remain unvaried, indicating that the intrinsic physics stays the same across the three epochs. In the broader multi-messenger context, this suggests that, despite the changing look in the optical band, the candidate neutrino-emitter blazar 5BZQ J1243+4043 is still characterized by the presence of intense external radiation fields and radiatively efficient accretion, typical of high-excitation radio galaxies, which may foster neutrino production.

Key words. black hole physics – neutrinos – galaxies: active – galaxies: jets – quasars: emission lines – quasars: individual: 5BZQ J1243+4043

1. Introduction

Active galactic nuclei (AGNs) are among the most luminous, persistent extragalactic sources in the Universe and are powered by accretion onto the central supermassive black hole (SMBH). Among them, the radio-loud subclass of blazars hosts highly relativistic jets pointed in the observer's line of sight. Blazars may exhibit optical spectral lines produced when photons emitted by the accretion disk interact with surrounding gas clouds. These include the fast-moving clouds of the broad-line region (BLR), located closer to the central black hole, and the slower-moving gas of the narrow-line region (NLR) farther out. The higher-velocity denser ($n_e \gtrsim 10^9\,\mathrm{cm}^{-3}$; Osterbrock & Ferland 2006) gas of the BLR is responsible for broad lines (with a full width at half maximum, FWHM, of $\gtrsim$1000 km s^{-1}) of permitted and semi-forbidden transitions. The slower and less dense NLR ($n_e \lesssim 10^6\,\mathrm{cm}^{-3}$; Longair 1994) give origin to narrow forbidden lines instead.

Within the AGN unification model (Urry & Padovani 1995; Urry et al. 2004), blazars are traditionally classified in BL Lacertae objects (BL Lacs) and flat spectrum radio quasars (FSRQs) based on the rest-frame equivalent width (EW) of the optical spectral lines, which measures the line strength compared to the underlying continuum. In this observational-based scheme, FSRQs display intense broad (EW > 5 Å) emission lines in their optical spectra, while BL Lacs lack emission lines or show only absorption and narrow emission lines (EW < 5 Å).

A more physically driven scenario based on the modes of accretion onto the central SMBH and the intrinsic power of the relativistic jet has been proposed in the literature (Ghisellini & Celotti 2001; Best & Heckman 2012; Giommi et al. 2012). This approach was also adopted in our first work on the physical properties of candidate neutrino-emitter blazars (Azzollini et al. 2025, hereafter, Paper PI). The accretion efficiency is traced by the ratio of the BLR luminosity in Eddington units, $L_{\mathrm{BLR}}/L_{\mathrm{Edd}}$ (Ghisellini et al. 2009, 2011b; Sbarrato et al. 2012, 2014). The radio power at 1.4 GHz, instead, traces the intrinsic jet's power (Best & Heckman 2012; Heckman & Best 2014; Padovani et al. 2022). Based on their intrinsic properties, high-excitation radio galaxies (HERGs) are characterized by intense external radiation fields, efficient accretion, and powerful jets that exceed these thresholds. In contrast, low-excitation radio galaxies (LERGs) show weak or absent optical emission lines, reflecting their inefficient accretion, weaker radiation fields, and reduced jet power. The proposed dividing thresholds are $L_{\mathrm{BLR}}/L_{\mathrm{Edd}} \sim 5 \times 10^{-4}$ (Ghisellini et al. 2010, 2011a) and $P_{1.4\,\mathrm{GHz}} \sim 10^{26}\,\mathrm{W\,Hz}^{-1}$ (Best & Heckman 2012). Following this physical classification,

⋆ Corresponding author:
alessandra.azzollini@uni-wuerzburg.de

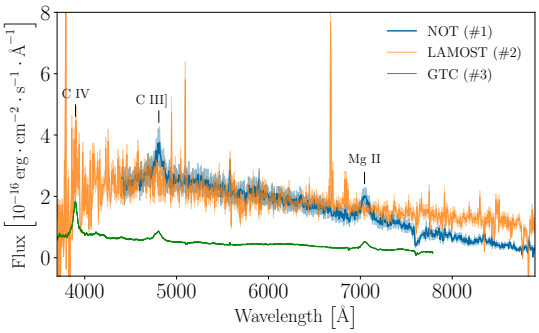

Fig. 1. Optical spectra of 5BZQ J1243+4043 from: the NOT spectrum #1 (MJD 56035.11; Titov et al. 2013) shown in blue, the LAMOST spectrum #2 (MJD 56360.75; Peña-Herazo et al. 2021a) in orange, and a new GTC spectrum #3 acquired in this work (MJD 60318.21) in green. The shaded areas indicate the corresponding flux uncertainties.

FSRQs and BL Lacs could be considered as the jetted counterparts of HERGs and LERGs, respectively.

In recent years, the empirical BL Lacs/FSRQs scenario has been called into question by blazars that transition between the two classes over time. These objects, referred to as changing-look blazars, exhibit emission lines in their optical spectra during some epochs, while appearing featureless at others (Vermeulen et al. 1995; Ghisellini et al. 2011b; Ruan et al. 2014; Peña-Herazo et al. 2021a; Ricci & Trakhtenbrot 2023). Several hypotheses have been proposed to explain this phenomenon. It could be associated with sudden changes in the accretion rate: broad spectral profiles appear (disappear) concurrently with the sudden increase (decrease) in the accretion rate (Xiao et al. 2022; Dong et al. 2025; Duffy et al. 2025). Alternatively, Doppler boosting may modify the intensity and beaming of the photo-ionizing continuum over time and, consequently, this affects the interplay with the thermal line emission. Some studies have shown that the EW of the BLR lines is anti-correlated with the continuum luminosity (Corbett et al. 2000; Ruan et al. 2014; Paiano et al. 2024). In this framework, the variable jet-driven non-thermal continuum can outshine the BLR emission, making the broad lines temporarily undetectable.

In Paper PI, we investigated the nature of the 52 blazars proposed as promising candidates of neutrino emission in Buson et al. (2022a,2022b hereafter Paper I) and Buson et al. 2023 (2023 hereafter, Paper II). Investigations of their HERG/LERG properties have revealed that the sample includes representatives of both classes, with a mild tendency toward HERG-like properties. In the lepto-hadronic scenario, the efficiency of photo-pion production, which is a key mechanism for neutrino production, is strongly influenced by the accretion mode. Identifying the presence of external radiation fields, such as those characteristic of HERGs, is therefore important when we are looking to interpret the physical conditions leading to neutrino emission.

The blazar 5BZQ J1243+4043 was part of that sample, it was proposed as the blazar counterpart of a γ-ray source in Principe et al. (2021) and was classified as a HERG based on optical spectra from 2012. However, prior studies have suggested it may be a changing-look blazar, exhibiting transitions between the FSRQ and BL Lac classes due to variability in its optical emission lines over time (Peña-Herazo et al. 2021b). This prompts the question of whether the observed spectral changes reflect a genuine evolution in the blazar's physical properties, requiring a reassessment of its HERG–LERG classification with implications for neutrino production or cosidering whether they might instead be the result of observational effects with limited physical implications.

In this paper, we focus on the optical spectroscopic properties of the blazar 5BZQ J1243+4043, using both archival and new optical spectra among three epochs. The work is organized as follows. Section 2 describes the dataset and analysis. Section 3 presents the findings. Section 4 summarizes our conclusions. We assumed a flat ΛCDM cosmology with $H_0 = 69.3\,\mathrm{km\,s^{-1}\,Mpc^{-1}}$, $\Omega_{m0} = 0.29$, and $\Omega_\Lambda = 0.71$.

2. Optical spectroscopy analysis

2.1. Optical spectroscopy dataset

Three optical spectra are available for 5BZQ J1243+4043 at different times spanning ∼12 years (shown in Fig. 1). A first spectrum was acquired with the Nordic Optical Telescope (NOT, blue) on April 18th, 2012 (MJD 56035.11, hereafter spectrum #1; Titov et al. 2013).

Based on the detection of prominent emission lines in spectrum #1, the blazar 5BZQ J1243+4043 was classified as FSRQ in the fifth edition of the Roma-BZCat catalog (5BZCat; Massaro et al. 2015), with a redshift of $z = 1.5181 \pm 0.0002$. This spectrum was used in Paper PI to determine the physical classification of 5BZQ J1243+4043, identifying it as an HERG.

A second spectrum was acquired on March 9th, 2013 (MJD 56360.75, hereafter spectrum #2; Peña-Herazo et al. 2021b) within the Large Sky Area Multi-Object Fiber Spectroscopic Telescope Survey (LAMOST; Zhao et al. 2012). This spectrum was pointed out as featureless and our analysis confirmed these earlier findings, based on the spectral components being narrower than the minimum width set by the instrument resolution.

We acquired a third spectrum on January 9th, 2024 (MJD 60318.21; hereafter, spectrum #3) with the R1000B grism of the Optical System for Imaging and low-Intermediate-Resolution Integrated Spectroscopy of the Gran Telescopio Canarias (GTC OSIRIS, green; Cepa et al. 2003). We reduced this spectrum using the `PypeIt v1.16.0` pipeline (Prochaska et al. 2020) following standard analysis procedures

2.2. Methodology for the estimation of physical properties

The three spectra were examined and used for further analysis following the same approach described in Paper PI. After extracting the three spectra, we applied a power-law fit $F_\lambda \propto \lambda^\alpha$ to the spectral continuum around the Mg II line profile (as in Pandey et al. 2025) to model the non-thermal radiation of the jet (Falomo et al. 1994; Urry & Padovani 1995; Scarpa & Falomo 1997; Corbin 1997; Ghisellini et al. 1998). We analyzed the identified emission lines and extracted the flux, EW, and FWHM. For the featureless spectrum #2, we estimated upper limits (ULs) on the undetected lines. The total luminosity of the emission lines (or the limit) was used to infer the accretion BLR luminosity L_{BLR} of the blazar. Furthermore, we used the lines' luminosity and FWHM to estimate the virial black hole mass and the Eddington luminosity as a result (as in Paper PI; see also Shen et al. 2011; McLure et al. 2004; Vestergaard & Osmer 2009. As in Paper PI, we used the radio flux density at 1.4 GHz from the NRAO VLA Sky Survey (NVSS, Condon et al. 1998) to determine the radio power that traces the intrinsic power of the relativistic jet.

2.3. Results

The continuum and line emission estimates are listed in Table 1 and displayed in Fig. 2 (see also Fig. B.1). In the NOT spectrum #1, we confirmed the detection of broad C III and Mg II

Table 1. Spectral properties of 5BZQ J1243+4043 across the three epochs.

Spectrum	Component	Flux	Rest-frame EW	FWHM
		10^{-16} erg cm^{-2} s^{-1} Å^{-1}	Å	km s^{-1}
NOT #1	Continuum	1.34 ± 0.24	–	–
	C III	3.47 ± 0.90	23.43 ± 2.11	6007.87 ± 90.12
	Mg II	2.01 ± 0.40	24.87 ± 2.98	6972.74 ± 146.43
LAMOST #2	Continuum	2.21 ± 0.49	–	–
	C IV	<1.26	–	4000.00 [a]
	C III	<1.72	–	4000.00 [a]
	Mg II	<1.35	–	4000.00 [a]
GTC #3	Continuum	0.30 ± 0.05	–	–
	C IV	0.66 ± 0.07	36.30 ± 4.36	4774.69 ± 42.97
	He II	0.25 ± 0.04	1.74 ± 0.14	1254.48 ± 3.76
	N III	0.77 ± 0.13	2.82 ± 0.23	1499.47 ± 7.50
	C III	0.96 ± 0.14	25.10 ± 3.26	6152.56 ± 86.14
	Mg II	0.53 ± 0.08	51.87 ± 10.37	5628.52 ± 157.60

Notes. The first column reports the reference spectrum. The second, third, fourth and fifth columns list the spectral component with corresponding flux, either measured or limits, rest-frame EW and FWHM. [a]In spectrum #2, we placed ULs on the undetected emission lines by fixing the FWHM (see Paper PI).

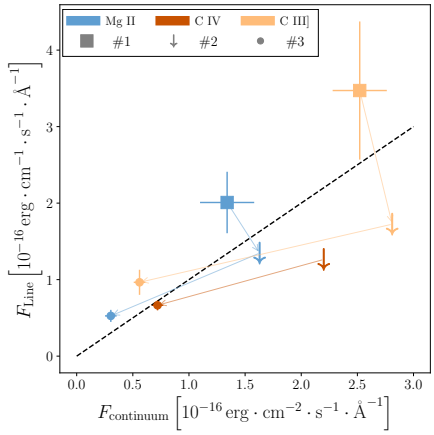

Fig. 2. Variations in the emission line fluxes as a function of the underlying continuum level across the three epochs of 5BZQ J1243+4043. The values for Mg II, C IV, and C III emission lines are indicated in blue, brown, and yellow, respectively. The values corresponding to spectra #1 and #3 are indicated with a square and a filled circle, respectively, while the arrows show the limits derived for epoch #2. The dotted black line traces the diagonal, corresponding to equality.

emission lines at 4796 and 7040 Å, respectively, consistent with the redshift $z = 1.5181 \pm 0.0002$ (Titov et al. 2013). The continuum is described by a power law with a flux of$(1.34 \pm 0.24) \times 10^{-16}$ erg cm^{-2} s^{-1} Å^{-1} and spectral index of $\alpha = -1.51 \pm 0.12$. Spectrum #2 appears featureless in terms of emission lines, consistent with the object exhibiting BL Lac characteristics at that time, thereby leading to its classification as a changing-look blazar. We identified two absorption components at ∼8766 and ∼8833 Å, likely corresponding to Fe I transitions (Meggers et al. 1961). This remains consistent with the non-detection of BLR lines. The continuum follows a power law with a flux of $(2.21 \pm 0.49) \times 10^{-16}$ erg cm^{-2} s^{-1} Å^{-1} and index of $\alpha = -1.00 \pm 0.24$. We placed an UL on the BLR line fluxes by simulating C IV, C III, and Mg II lines.

In the newly acquired spectrum #3, we identified C IV at 3898 Å, He II 1640 Å at 4128 Å, N III 1750 Å at 4405 Å, C III 1909 Å at 4802 Å, and Mg II 2798 Å at 7046 Å. These results confirm the redshift value $z = 1.5181 \pm 0.0002$. The Mg II profile shows two double absorption components on its blue wing, at 6871−6890 Å and 6975−6993 Å, respectively, which might be associated with the interstellar medium (ISM) of the host galaxy, with intervening absorbing material from massive galaxies nearby and/or the presence of wind outflowing from the disk (Santoro et al. 2018, 2020; Paiano et al. 2024; Chen & Ho 2025). The continuum follows a power-law of flux $(0.30 \pm 0.05)\times 10^{-16}$ erg cm^{-2} s^{-1} Å^{-1} and index $\alpha = -1.50 \pm 0.08$.

3. Discussion

The three observations of 5BZQ J1243+4043 used in this study point toward a variation in the BLR luminosity over ∼12 yr, with a gradual decrease of the line luminosities while the accretion regime remains, overall, unvaried. We observed variations in both the continuum and line emission, as evident from Fig. 2. The continuum flux increases from spectrum #1 to spectrum #2, when it reaches its maximum coincident with a featureless optical spectrum; then it decreases again in spectrum #3. A first implication of the observed spectral variability is that this blazar is not characterized by a straightforward disk–jet relation: when BLR lines are detected, in epoch #1 and #3, both the line and the continuum flux drop, while the corresponding EW increases. This suggests that the continuum (i.e., the jet emission) decreases more rapidly than the line (disk) emission. During the higher jet state, #2, the question of whether the BLR lines are outshone or their absence reflects a drop in the disk luminosity (and, hence, a change in the radiation field properties) remains open. To study this, we performed a test simulation to investigate the impact of spectral lines as bright as those observed in #1 and #3 over a continuum as high as spectrum #2; namely, the highest observed for this blazar and with no evidence of lines. As shown in Figs. A.1 and A.2, we found that the presence of BLR lines as luminous and broad as those detected in #1 and #3 is not excluded in spectrum #2. If present, they would be outshone by the optical continuum flux, likely dominated by the non-thermal component. An overall higher jet activity contemporaneous with epochs #1 and #2 is consistent with the γ-ray detection of the blazar during 2008–2019 Principe et al. (2021) and its non-inclusion in more recent *Fermi*-LAT catalogs (Ballet et al. 2023).

Despite the observed variability in the line and continuum emission across the three epochs, the accretion properties and, more generally, the underlying physics, ultimately remain the same. This is traced by the $L_{\rm BLR}/L_{\rm Edd}$ ratio, which lies above the dividing line for 5BZQ J1243+4043 ($L_{\rm BLR}/L_{\rm Edd} \sim 5 \times 10^{-4}$; Ghisellini et al. 2011b; Best & Heckman 2012; Sbarrato et al. 2014). In other words, it displays HERG-like properties: the ratio is $L_{\rm BLR}/L_{\rm Edd} \sim 1.30 \times 10^{-3}$ in #1 and $\sim 1.43 \times 10^{-3}$ in #3. In epoch #2, the ULs result in $L_{\rm BLR}/L_{\rm Edd} \lesssim 7.19 \times 10^{-3}$. Similarly, the jet power of this blazar is $P_{1.4\,\rm GHz} \sim 2.91 \times 10^{27}$ W Hz^{-1}, above the corresponding threshold $P_{1.4\,\rm GHz} \simeq 10^{26}$ W Hz^{-1} (Best & Heckman 2012; Padovani et al. 2022), which corroborates its HERG-like nature. This is also shown in Fig. 3, which represents the accretion regime $L_{\rm BLR}/L_{\rm Edd}$ as a function of $P_{1.4\,\rm GHz}$. The values of three epochs (#1 as a blue square, #2 as an orange arrow, and #3 as a green dot) of 5BZQ J1243+4043 are overlaid to those of the candidate neutrino-emitter blazar sample and other reference blazar samples investigated in Paper PI (gray). Horizontal dashed and vertical dashed-dotted lines indicate the LERG−HERG thresholds.

This shows that despite the observed spectral variability, the nature of the candidate neutrino-emitter blazar 5BZQ J1243+4043 remains consistent with radiatively efficient accretion, intense external radiation fields, and high jet power across the ∼12 yr. This is consistent with the mild tendency

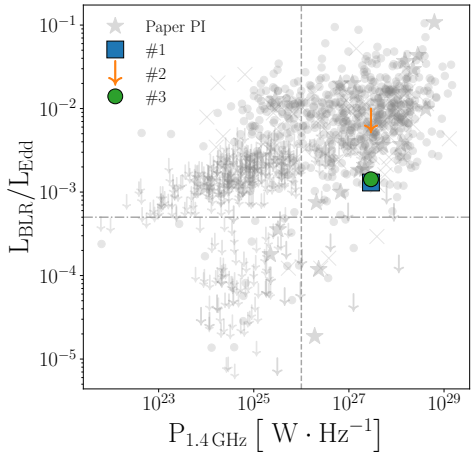

Fig. 3. Accretion regime L_{BLR}/L_{Edd} as a function of the radio power at 1.4 GHz. The three considered epochs (#1 as a blue square, #2 as an orange arrow, #3 as a green dot) of 5BZQ J1243+4043 are compared to the blazar samples analyzed in Paper PI (gray). The horizontal dotted and vertical dashed-dotted black lines represent the boundaries for the LERG/HERG-like behavior, respectively. As discussed in Sect. 3, despite the line emission variations, the object remains in the radiative-efficient regime.

toward HERG-like properties found for the full sample of neutrino candidates (Paper PI; see also Paper I and Paper II).

4. Summary and conclusions

In this work, we studied the behavior of the blazar 5BZQ J1243+4043, which was recently proposed as a candidate for IceCube neutrinos and as a changing-look blazar in the literature, among three epochs covered by optical spectroscopy observations. We used new data acquired with the Gran Telescopio Canarias for the third epoch. We analyzed the properties of the emission lines detected in the first and third spectra and placed limits on the nondetections during the second epoch. We compared their flux with the continuum in all three cases.

Our analysis shows that the highest continuum coincides with a featureless spectrum. However, this is not inconsistent with the presence of BLR lines, as observed for the other two epochs. We observed spectral variability in both the continuum and emission lines, with the decrease in the line intensities between the first and third epoch accompanied by an increase in the corresponding equivalent width and a slight hardening of the spectral index.

Our findings show that while observational properties vary across the three epochs, the underlying physical properties remain the same. Among the three considered epochs, the candidate neutrino-emitter blazar 5BZQ J1243+4043 is characterized by intense external radiation fields, a radiatively efficient accretion regime, and powerful jets that are typical of HERG-like sources. This is particularly important in the broader multi-messenger context, since 5BZQ J1243+4043 has been pointed out as a promising candidate for the long-term emission of IceCube neutrinos (Paper II). The combination of efficient particle acceleration and the presence of intense external radiation fields might indeed foster neutrino production in the powerful jet of efficiently accreting blazars, despite the observed variations in the appearance of spectral lines in the optical band.

Acknowledgements. We thank the anonymous referee for the constructive feedback. We thank Jose Maria Sanchez Zaballa and Leonard Pfeiffer for the insightful comments and fruitful discussions. This work was supported by the European Research Council, ERC Starting grant *MessMapp*, S.B. Principal Investigator, under contract no. 949555. This work is (partly) based on data obtained with the instrument OSIRIS, built by a Consortium led by the Instituto de Astrofísica de Canarias in collaboration with the Instituto de Astronom?a of the Universidad Autónoma de México. OSIRIS was funded by GRANTECAN and the National Plan of Astronomy and Astrophysics of the Spanish Government.

References

Azzollini, A., Buson, S., Coleiro, A., et al. 2025, A&A, 700, A228
Ballet, J., Bruel, P., Burnett, T. H., Lott, B., & The Fermi-LAT Collaboration 2023, ArXiv e-prints [arXiv:2307.12546]
Best, P. N., & Heckman, T. M. 2012, MNRAS, 421, 1569
Buson, S., Tramacere, A., Oswald, L., et al. 2023, ArXiv e-prints [arXiv:2305.11263]
Buson, S., Tramacere, A., Pfeiffer, L., et al. 2022a, ApJ, 933, L43
Buson, S., Tramacere, A., Pfeiffer, L., et al. 2022b, ApJ, 934, L38
Cepa, J., Aguiar-Gonzalez, M., Bland-Hawthorn, J., et al. 2003, in Instrument Design and Performance for Optical/Infrared Ground-based Telescopes, eds. M. Iye, & A. F. M. Moorwood, SPIE Conf. Ser., 4841, 1739
Chen, Z.-F., & Ho, L. C. 2025, ApJ, 980, 159
Condon, J. J., Cotton, W. D., Greisen, E. W., et al. 1998, AJ, 115, 1693
Corbett, E. A., Robinson, A., Axon, D. J., & Hough, J. H. 2000, MNRAS, 311, 485
Corbin, M. R. 1997, ApJ, 485, 517
Dong, Q., Zhang, Z. X., Gu, W. M., Sun, M., & Zheng, Y. G. 2025, ApJ, 986, 160
Duffy, L., Eracleous, M., Ruan, J. J., Yang, Q., & Runnoe, J. C. 2025, ApJ, 989, 102
Falomo, R., Scarpa, R., & Bersanelli, M. 1994, ApJS, 93, 125
Ghisellini, G., & Celotti, A. 2001, A&A, 379, L1
Ghisellini, G., Celotti, A., Fossati, G., Maraschi, L., & Comastri, A. 1998, MNRAS, 301, 451
Ghisellini, G., Maraschi, L., & Tavecchio, F. 2009, MNRAS, 396, L105
Ghisellini, G., Tavecchio, F., Foschini, L., et al. 2010, MNRAS, 402, 497
Ghisellini, G., Tagliaferri, G., Foschini, L., et al. 2011a, MNRAS, 411, 901
Ghisellini, G., Tavecchio, F., Foschini, L., & Ghirlanda, G. 2011b, MNRAS, 414, 2674
Giommi, P., Padovani, P., Polenta, G., et al. 2012, MNRAS, 420, 2899
Heckman, T. M., & Best, P. N. 2014, ARA&A, 52, 589
Longair, M. S. 1994, High Energy Astrophysics. Vol. 2: Stars, the Galaxy and the Interstellar Medium (Cambridge: Cambridge University Press), 2
Massaro, E., Maselli, A., Leto, C., et al. 2015, Ap&SS, 357, 75
McLure, R. J., & Dunlop, J. S. 2004, in Multiwavelength AGN Surveys, eds. R. Mújica, & R. Maiolino, 389
Meggers, W. F., Corliss, C. H., & Scribner, B. F. 1961, Tables of Spectral-line Intensities
Osterbrock, D. E., & Ferland, G. J. 2006, Astrophysics Of Gas Nebulae and Active Galactic Nuclei (University Science books)
Padovani, P., Giommi, P., Falomo, R., et al. 2022, MNRAS, 510, 2671
Paiano, S., Falomo, R., Treves, A., Scarpa, R., & Sbarufatti, B. 2024, ApJ, 968, 81
Pandey, A., Hu, C., Wang, J.-M., et al. 2025, ApJ, 978, 120
Peña-Herazo, H. A., Massaro, F., Gu, M., et al. 2021a, AJ, 161, 196
Peña-Herazo, H. A., Paggi, A., García-Pérez, A., et al. 2021b, AJ, 162, 177
Principe, G., Di Venere, L., Orienti, M., et al. 2021, MNRAS, 507, 4564
Prochaska, J., Hennawi, J., Westfall, K., et al. 2020, J. Open Source Softw., 5, 2308
Ricci, C., & Trakhtenbrot, B. 2023, Nat. Astron., 7, 1282
Ruan, J. J., Anderson, S. F., Plotkin, R. M., et al. 2014, ApJ, 797, 19
Santoro, F., Rose, M., Morganti, R., et al. 2018, A&A, 617, A139
Santoro, F., Tadhunter, C., Baron, D., Morganti, R., & Holt, J. 2020, A&A, 644, A54
Sbarrato, T., Ghisellini, G., Maraschi, L., & Colpi, M. 2012, MNRAS, 421, 1764
Sbarrato, T., Padovani, P., & Ghisellini, G. 2014, MNRAS, 445, 81
Scarpa, R., & Falomo, R. 1997, A&A, 325, 109
Shen, Y., Richards, G. T., Strauss, M. A., et al. 2011, ApJS, 194, 45
Titov, O., Stanford, L. M., Johnston, H. M., et al. 2013, AJ, 146, 10
Urry, C. 2004, in AGN Physics with the Sloan Digital Sky Survey, eds. G. T. Richards, & P. B. Hall, ASP Conf. Ser., 311, 49
Urry, C. M., & Padovani, P. 1995, PASP, 107, 803
Vermeulen, R. C., Ogle, P. M., Tran, H. D., et al. 1995, ApJ, 452, L5
Vestergaard, M., & Osmer, P. S. 2009, ApJ, 699, 800
Xiao, H., Fan, J., Ouyang, Z., et al. 2022, ApJ, 936, 146
Yao, S., Liu, C., Zhang, H.-T., et al. 2012, Res. Astron. Astrophys., 12, 772
Zhao, G., Zhao, Y., Chu, Y., Jing, Y., & Deng, L. 2012, ArXiv e-prints [arXiv:1206.3569]

Appendix A: Test simulation of the emission lines

We aim to investigate the line variability across the three epochs of 5BZQ J1243+4043. To this end, we simulated a Gaussian profile corresponding to a Mg II and C III emission lines with the same flux, EW and FWHM as the ones observed in spectra #1 and #3. Then, we compared their brightness to a continuum as high and hard as in spectrum #2, i.e., the highest observed for this blazar and with no evidence of lines. The result is shown in Figs. A.1-A.2, which shows the spectrum #2 in orange, and the Gaussians corresponding to the Mg II and C III fluxes of #1/#3 in blue/green, respectively. The shaded areas indicate the corresponding 1σ uncertainties on the flux.

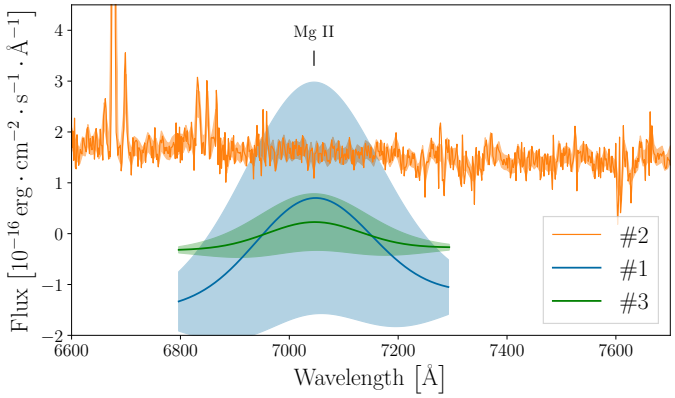

Fig. A.1. Test simulation of a Mg II as bright and broad as in spectra #1 (blue) and #3 (green) over a continuum as high as in #2 (orange). The shaded areas show the corresponding 1σ uncertainties.

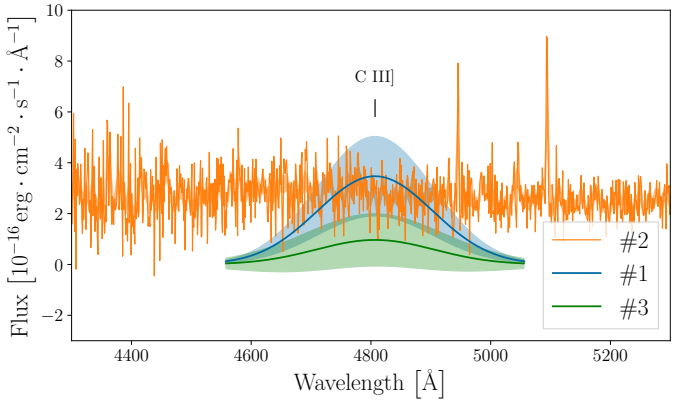

Fig. A.2. Test simulation of a C III as bright and broad as in spectra #1 (blue) and #3 (green) over a continuum as high as in #2 (orange). The shaded areas show the corresponding 1σ uncertainties.

This result shows that if lines as bright as those seen in spectra #1/#3 are present, they would be outshone by the higher jet continuum.

Appendix B: The fit of the continuum

As explained in Sect. 2.2, we applied a power-law fit to the spectral continuum around the Mg II line profile to investigate the changes in the non-thermal radiation of the jet across the three epochs. The results are reported in Table 1, and shown in Fig. B.1.

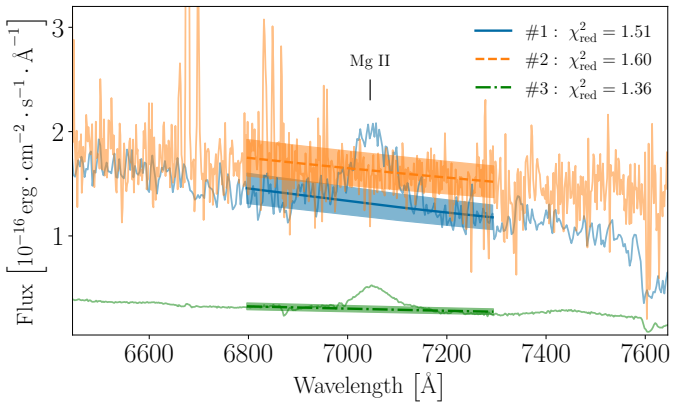

Fig. B.1. Power-law fit of the spectral continuum in the three epochs of 5BZQ J1243+4043 with the corresponding reduced χ^2_{red}: #1 shown in solid blue, #2 in dotted orange, and #3 in dash-dotted green. The shaded areas indicate the corresponding flux uncertainties.

Appendix C: Journal of observations

Table C.1 provides further details on the spectral dataset used for the analysis. The three observations were performed under the same conditions of slit width greater than or similar to the seeing, ensuring a reliable flux calibration and estimation[1] (Titov et al. 2013; Yao et al. 2012).

Table C.1. Observational details of the spectral dataset.

Spectrum	Instrument	Resolution	Observation date [MJD]	$\mathbf{t}_{\mathrm{exp}}$ [ks]
#1	NOT ALFOSC[1]	415	56035.11	2.40
#2	LAMOST[2]	1000	56360.75	6.37
#3	GTC OSIRIS	1018	60318.21	3.00

Notes. The first column reports the reference spectrum. The second, third, fourth and fifth columns list the observation details with corresponding instrument, resolution $R = \lambda/\Delta\lambda$, observation date and total exposure time.
(1)From Titov et al. (2013) (2)From Peña-Herazo et al. (2021a)

[1] For further details on GTC OSIRIS see, for example, https://atmosportal.gtc.iac.es and https://www.gtc.iac.es/instruments/osiris+/osiris+.php.